Available online at www.sciencedirect.com
SCIENCE DIRECT®
Carbohydrate Polymers 54 (2003) 149–158
Carbohydrate Polymers
www.elsevier.com/locate/carbpol

High resolution imaging of the microstructure of maize starch films

Rossana M.S.M. Thiré[a], Renata A. Simão[a], Cristina T. Andrade[b,*]

[a]*PEMM/COPPE, Universidade Federal do Rio de Janeiro, P.O. Box 68505, 21945-970 Rio de Janeiro, Brazil*
[b]*Instituto de Macromoléculas Professora Eloisa Mano, Universidade Federal do Rio de Janeiro, P.O. Box 68525, 21945-970 Rio de Janeiro, Brazil*

Received 9 December 2002; revised 8 April 2003; accepted 14 April 2003

Abstract

Glycerol-plasticised and non-plasticised cast films were prepared from maize starch suspensions that had been heated under reflux for different periods of time. Light microscopy (LM) and atomic force microscopy (AFM) have been used to observe the morphology of the starch films. In general, LM and AFM topographic images of corresponding non-plasticised films were similar. AFM topographic images of plasticised films revealed differences associated with the retarding effect of glycerol on the gelatinisation process. Relatively high B-type crystallinity indices were determined for plasticised films, independently of the heating conditions to which the suspensions had been submitted. AFM topographic images of plasticised films at higher magnifications revealed smooth and rough domains, that were detailed by phase contrast imaging.

Keywords: Maize starch; Atomic force microscopy; Film formation; Gelatinisation; Retrogradation; Microstructure; Phase separation

1. Introduction

In the last decade, there has been a growing interest in the development of thermoplastic materials from biodegradable polymers, especially those derived from renewable resources. Among them, starch has received much attention because it is a low-cost, worldwide available product (Bastioli, 1998; Lörks, 1998; Shogren, 1993).

Starch occurs as semi-crystalline granules in grains, roots and tubers, and is composed of a mixture of D-glucan macromolecules, amylose and amylopectin. Amylose is an essentially linear α-(1,4)-linked D-glucan. Amylopectin is the highly branched component of starch with α-(1,6)-linked branch points. The granule crystallinity is associated with the amylopectin linear chains and may give different X-ray diffraction (XRD) patterns, depending on the starch source. Cereal starches produce an A-crystalline pattern (monoclinic lattice) with densely packed double helices in the unit cell (Imberty, Chanzy, Pérez, Buléon, & Tran 1988). Potato and certain tuber starches give a B-crystalline pattern (hexagonal lattice) in which the double helices packed in parallel fashion are combined with structured water (Imberty & Pérez, 1988). C-crystalline pattern is an intermediate form and occurs in certain legume starches.

Microscopic techniques have been used to investigate the structure of starch granule, in which 120–400 nm thick alternating amorphous and semi-crystalline growth rings are arranged (French, 1984; Yamaguchi, Kainuma, & French, 1979). Although little is known regarding the molecular organisation in amorphous rings, experimental results obtained from studies on semi-crystalline rings are rather conclusive. Semi-crystalline rings consist of alternating amorphous and crystalline lamellae. Amylopectin linear chains, through ordered arrangements of double helices form the so-called clusters, which give rise to crystalline lamellae. Amylopectin branching points and amylose form the amorphous regions (Jenkins, Cameron, & Donald, 1993; Kassenbeck, 1975, 1978; Oostergetel & van Bruggen, 1989). Spherical blockets with diameter varying in the range 20–500 nm, depending on the starch type and location in the granule, have been suggested as a new level of granule organisation between that of lamellae and growth rings (Gallant, Bouchet, & Baldwin, 1997).

Native granular starch is converted into a thermoplastic material by conventional methods in the presence of plasticisers, such as water and glycerol. Starch films can be prepared from dilute suspensions by casting.

* Corresponding author. Tel.: +55-21-25627033; fax: +55-21-25621317.
E-mail address: ctandrade@ima.ufrj.br (C.T. Andrade).

0144-8617/03/$ - see front matter © 2003 Elsevier Ltd. All rights reserved.
doi:10.1016/S0144-8617(03)00167-X

Gelatinisation, melting, gelation and retrogradation are important phenomena involved in the processing of native starches. Gelatinisation and melting are related phenomena, during which the crystalline and molecular orders of native starch are disrupted. The gelatinisation process that takes place by heating under moderate shear in excess water is characterised by hydration, swelling, and loss of birefringence and crystallinity, as extensively studied by many techniques, such as differential scanning calorimetry (DSC) (Donovan, 1979; Jang & Pyun, 1996), high resolution ^{13}C solid state NMR spectroscopy (^{13}C CP MAS NMR) (Cooke & Gidley, 1992), and by combined small- and wide-angle X-ray scattering, DSC and small-angle neutral scattering (SAXS/WAXS/DSC/SANS) (Jenkins & Donald, 1998). During swelling, leaching of amylose out of the granules is partially responsible for the increase in viscosity of the starch suspension (Miller, Derby, & Trimbo, 1973). Partially because the swollen granule may remain insoluble and undamaged, and also contributes to the paste viscosity. Many studies were devoted to investigate the remaining part of the granule, or ghost, composed at least primarily of amylopectin molecules (Atkin, Abeysekera, Cheng, & Robards, 1998a; Atkin, Abeysekera, & Robards, 1998b; Derek, Prentice, Stark, & Gidley, 1992; Fannon & BeMiller, 1992; Obanni & BeMiller, 1996). Gelation of starch may be defined as the rapid formation of a three-dimensional network by leached amylose molecules, that occurs on cooling of the hot paste (Gidley, 1989). In contrast, retrogradation was shown to involve amylose and amylopectin re-crystallization on storage of gelled pastes (Keetels, Oostergetel, & van Vliet, 1996; Miles, Morris, Orford, & Ring, 1985), starch films (Rindlav, Hulleman, & Gatenholm, 1997), and thermoplastic starch-based materials (Hulleman, Kalisvaart, Janssen, Feil, & Vliegenthart, 1999; van Soest, Hulleman, de Witt, & Vliegenthart, 1996).

Atomic force microscopy (AFM) is a technique that provides direct spatial mapping of surface topography and surface heterogeneity with nanometre resolution without any specific sample preparation conditions (Garcia & Pérez, 2002; Raghavan, Gu, Nguyen, VanLandingham, & Karim, 2000). AFM has been used to examine the surface and internal structure of starch granules (Baker, Miles, & Helbert, 2001; Baldwin, Davies, & Melia, 1997; Krok, Szymonska, Tomasik, & Szymonski, 2000; Ridout, Gunning, Parker, Wilson, & Morris, 2002) and the surface of extruded films (Kuutti, Peltonen, Myllärinen, Teleman, & Forssell, 1998; Raghavan & Emekalam, 2001). However, to our knowledge, no investigation of surface morphology of starch films prepared by casting has been conducted by this technique.

In the present work, AFM and light microscopy (LM) were used to investigate the surface morphology of glycerol-plasticised and non-plasticised maize starch films prepared by casting from suspensions submitted to different gelatinisation times. Some XRD data are also presented. The results are expected to contribute to a better understanding of the properties of starch films.

2. Materials and methods

2.1. Preparation of films

Food grade maize starch was supplied by Corn Products (São Paulo, Brazil). Maize starch (5 g) was dispersed in 50 ml distilled and deionised water at room temperature. Suspensions were diluted with 50 ml water previously heated to 95 °C and then kept under stirring and reflux conditions for different periods of time. Glycerol (0.75 g) was added as a plasticiser to some suspensions. The hot suspensions were poured onto Petri dishes and allowed to dry at 50 °C for 12 h. Films were peeled off and conditioned for 10 days at 50% relative humidity (RH) before measurements. Starch suspensions plasticised with glycerol that were heated for 5, 20 and 90 min gave rise to films that have been called 5MG, 20MG and 90MG, respectively. Similarly, 5M, 20M, 50M and 90M designate films prepared from water suspensions without glycerol and that were heated for 5, 20, 50 and 90 min, respectively. The thickness of the films (70–100 μm) was measured with a digital micrometer. At least three specimens of each type were prepared and analysed by LM and AFM.

2.2. Atomic force microscopy

A Topometrix Accurex II (Topometrix, Santa Clara, USA) instrument, equipped with a non-contact AFM probe head and a 100 μm Tripot scanner was used to image the samples. The tips (Topometrix 1660™) were made of silicon and mounted on a cantilever with a spring constant of ca. 40 N/m and resonance frequencies in the 100–150 kHz range. Scanning was carried out at the free cantilever oscillation frequency and different amplitudes, depending on the stability and contrast obtained. The amplitude was set higher than 80 nm and the set point was fixed at 10–30% of the free oscillation amplitude in order to guarantee that the microscopy was operating in intermittent contact mode. Samples were fixed on double-coated adhesive tapes and the AFM images of the upper surface were obtained in air. Changes in the sample vertical position are presented as height images. Changes in the phase angle difference between the oscillations of the cantilever and the standard signal, which drives the piezoelectric crystal during the intermittent contact mode, are presented as phase images. The Global Lab® Image software (SPO550) (Data Translation Malboro, USA) was used to process images.

2.3. Light microscopy

An Olympus BX60M optical microscope (Olympus America Inc., New York, USA) was used to image the samples at several magnifications.

2.4. X-ray diffraction

Maize starch films were analysed by XRD on a Miniflex diffractometer (Rigaku Corporation, Japan) operating at Cu Kα wavelength of 1.542 A. Data were acquired in the angular region (2θ) of 5–30° (step size of 0.05°, time per step of 1 s).

3. Results and discussion

Maize starch water suspensions were heated for 5–90 min in the presence of glycerol or without adding glycerol and dried in an oven at 50 °C, giving rise to plasticised and non-plasticised films. Figs. 1 and 2 show LM and AFM images of typical regions on surfaces of 5M, 20M, 50M and 90M non-plasticised films obtained from suspensions which had been submitted to heating for 5, 20, 50 and 90 min, respectively. In Figs. 1(a) (LM) and 2(a) (AFM), the surfaces of the resulting 5M films consist of a continuous matrix with irregularly spaced features with varied shapes and sizes. Since starch suspensions had been heated under reflux, leaching of a great amount of amylose molecules out of the granules could be inferred. However, under the stirring conditions used in the experiment, heating for 5 min was not sufficient to promote complete rupture of the granules.

Film formation involves a drying step, known to cause a certain degree of collapse or flattening of the structure of flexible polysaccharide molecules as the last layer of solvent evaporates (Stokke & Elgsaeter, 1991). However, the water-holding capacity of the starch molecules has a significant effect on the observed images, since many features maintain a nearly round shape. An average roundness index (value that indicates how closely the shape of a particle resembles a circle) of 0.79 was determined with Global Lab® Image software.

In this work, particles resulting from partial dissolution of starch and that resemble the original starch granules in shape are referred as granular envelopes; the term ghost is used to nominate withered granular envelopes.

In Figs. 1(a) and 2(a), it seems reasonable to conclude that the visualised surface features consist of granular envelopes, in average 10.7 μm in major axis and 7.2 μm in minor axis, surrounded by a matrix composed mostly of amylose (Derek et al., 1992; Fannon & BeMiller, 1992).

Suspensions without glycerol heated for 20 min gave rise to 20M films imaged in Figs. 1(b) and 2(b), in which ghosts of greater dimensions and ghosts remnants are visualised. As observed, the continuous heating under reflux for longer periods of time was expected to promote the increase of swelling and disruption of some ghost structures.

In Fig. 1(a) and (b), some granular envelopes on the surfaces of 5M and 20M films are enclosed inside a thick outer layer (indicated by arrows). Such structures, denominated as ‘walls’, were previously visualised in a lightly

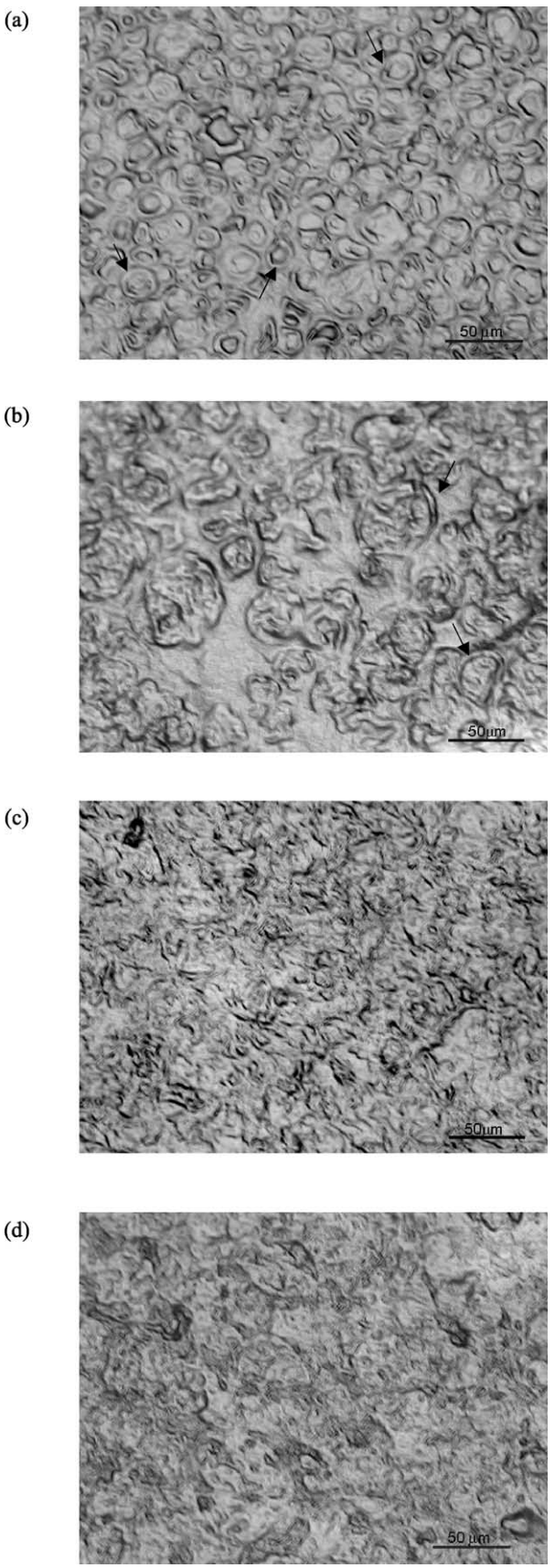

Fig. 1. Light micrographs of non-plasticised maize starch films: (a) 5M, (b) 20M, (c) 50M, and (d) 90M. Scale bar = 50 μm.

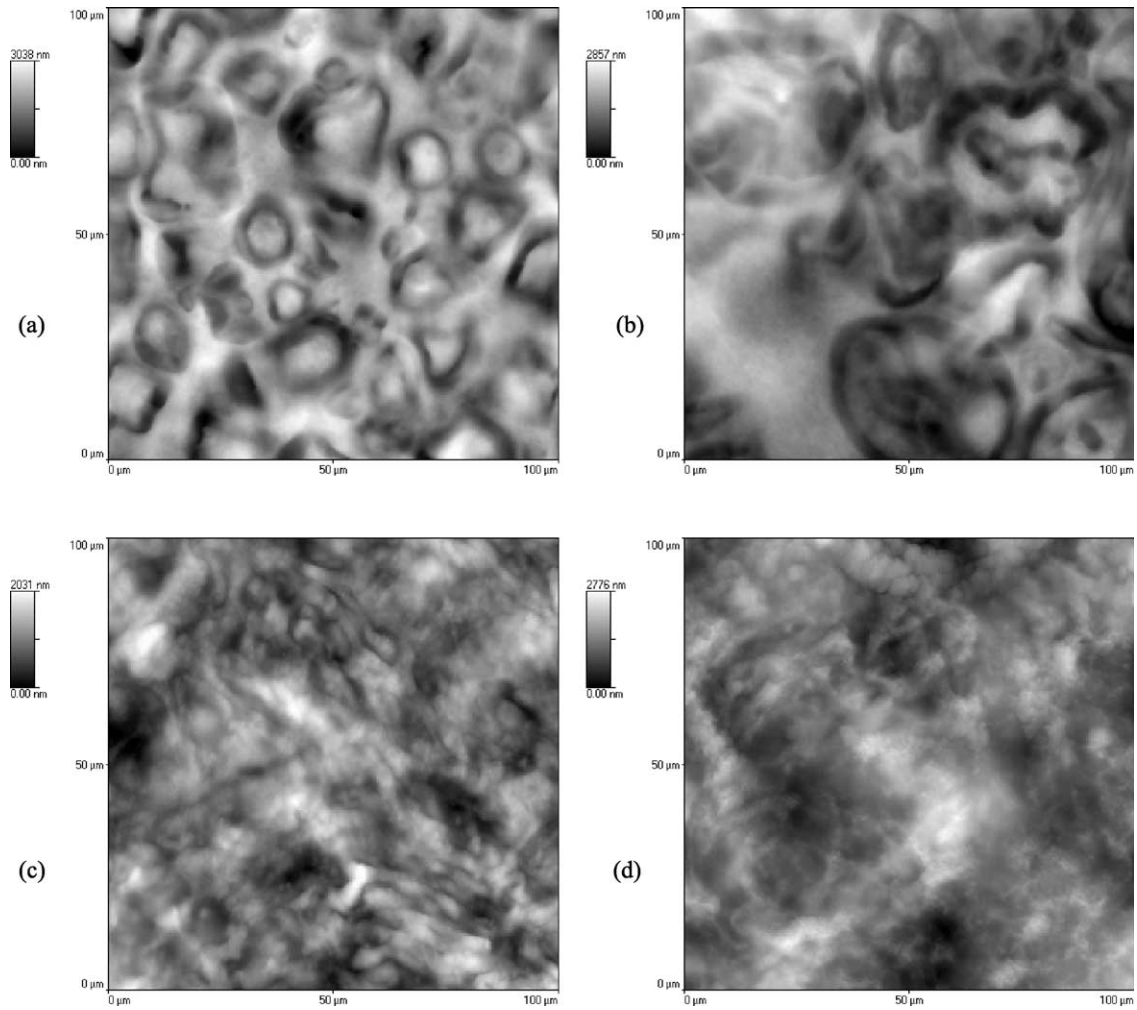

Fig. 2. AFM topographic images of non-plasticised maize starch films: (a) 5M, (b) 20M, (c) 50M, and (d) 90M.

cross-linked maize starch paste by low-temperature scanning electron microscopy (Fannon & BeMiller, 1992). In contrast, both AFM topographic images of Fig. 2(a) and (b) show that granular envelopes and ghosts are encircled by a depression (dark regions), instead of a wall. Such a depression may reflect the surface tension developed by concentrated amylose solutions in relation to granule remnants as the liquid evaporates during the process of film formation, or may be related to the limited miscibility (Kalichevsky & Ring, 1987) between amylose, present in the continuous matrix and amylopectin, which constitute the ghost outer layer (Derek et al., 1992).

The surfaces of 50M (Figs. 1(c) and 2(c)) and 90M (Figs. 1(d) and 2(d)) films are more homogeneous; swollen ghosts are not identified, since they had been fractured during prolonged heating. These images are consistent with that reported for fully gelatinised potato starch paste (Hermansson & Svegmark, 1996).

In general, the similarity between LM and AFM images confirms that AFM is a reliable technique to investigate the surface of starch bioplastic materials.

Glycerol-plasticised films were prepared and visualised by AFM. Fig. 3 shows topographic images of these films obtained from maize starch suspensions submitted to heating for 5, 20 and 90 min. In addition to water, glycerol is often used as a plasticiser to control the process and properties of starch-based thermoplastic materials. Glycerol has been shown to facilitate the gelatinisation of starch granules as effectively as water, although at a higher temperature (Perry & Donald, 2000). In the present case, gelatinisation was carried out in excess water under the same thermal conditions and glycerol was added at 15% (w/w) concentration in relation to starch. Addition of glycerol at this concentration was not expected to affect starch gelatinisation. Films obtained from suspensions that were heated for 5 min show similar morphologies (Figs. 2(a) and 3(a)), no matter what the solvent composition. In 5MG films, granular envelopes present approximately the same average dimensions (11 μm in minor axis, 17 μm in major axis and 0.9 μm in height) observed for 5M films. The same depression around the granular envelopes is visualised.

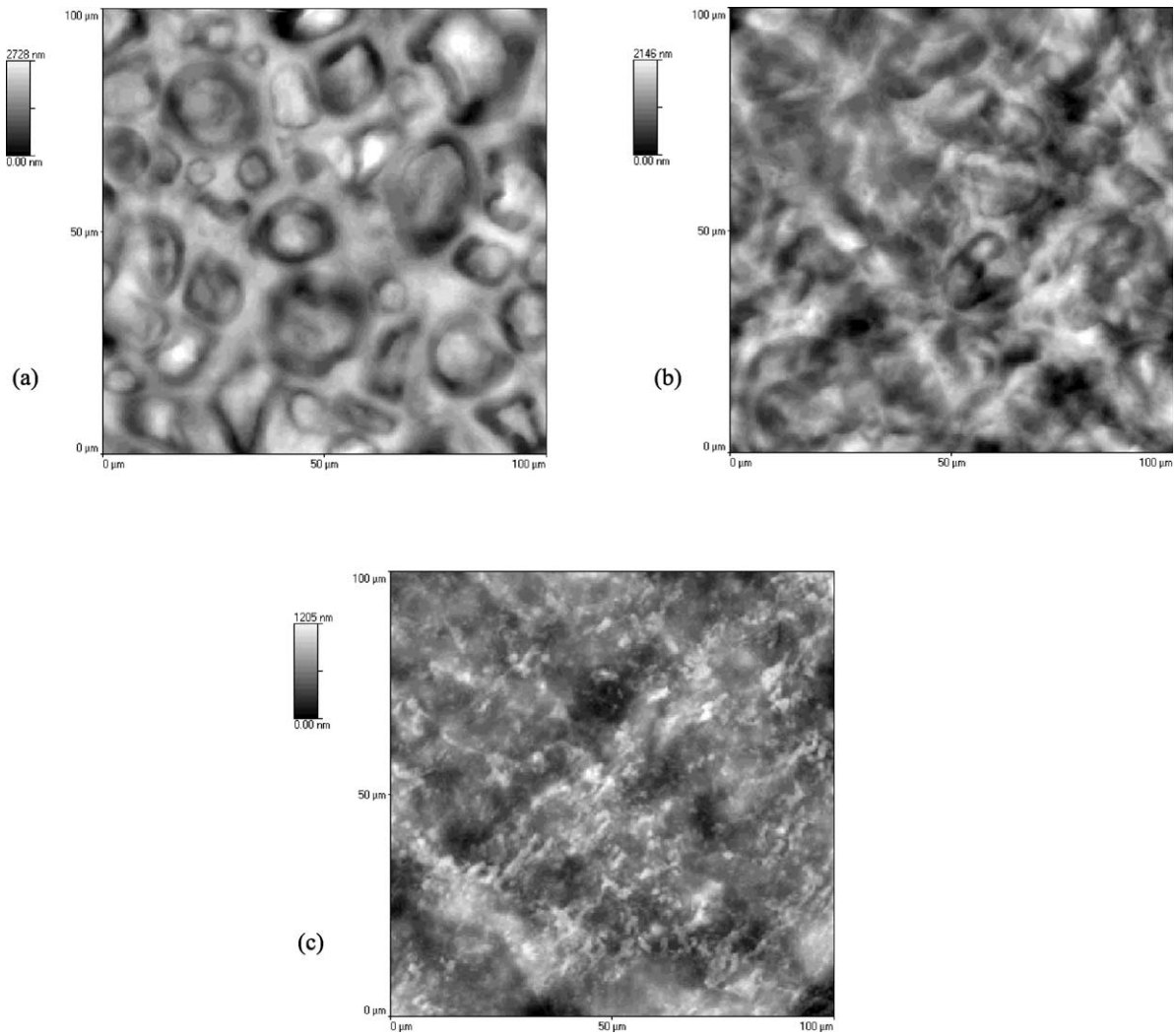

Fig. 3. AFM topographic of plasticised maize starch films: (a) 5MG, (b) 20MG, and (c) 90MG.

Comparing the AFM topographic images of Figs. 2(b) and 3(b), a smaller area, corresponding to the amylose matrix, is observed for the 20MG film (Fig. 3(b)) in relation to the 20M film (Fig. 2(b)). This result indicates that the suspension, which gave rise to the 20MG film should be in a less advanced stage of gelatinisation than that of the 20M film, which is consistent with the retarding effect of glycerol on the process. Heating starch suspensions for 90 min in the presence of glycerol gave rise to 90MG films, imaged in Fig. 3(c) as a more homogenous surface, in comparison with the previous surfaces of 5MG and 20MG films.

The development of crystallinity in starch gels, films and starch-based materials have been studied by several authors. Preparation conditions, such as temperature, RH and time of the drying procedure, were shown to affect the crystallinity of potato starch films. B-type crystallinity, varying from almost none to 23%, developed upon film formation, as determined by XRD (Rindlav et al., 1997). The effect of film formation conditions on the crystallinity of amylose and amylopectin from potato, with or without the addition of glycerol had been also investigated. Amylose films with or without the addition of glycerol as a plasticiser exhibited a relatively high degree of B-type crystallinity, whereas the non-plasticised amylopectin films were amorphous. Glycerol-plasticised amylopectin formed B-type crystallinity, depending on the RH conditions during film formation (Rindlav-Westling, Stadin, Hermansson, & Gatenholm, 1998). In the present work, the crystallinity of glycerol-plasticised maize films was investigated. Fig. 4 shows the X-ray diffractograms obtained for 5MG (trace a) and 90MG (trace b) films. As expected, the A-type crystallinity of native maize starch was not retained. Both 5MG and 90MG films displayed B-type crystalline patterns, with no significant differences. In these diffractograms, B-type crystallinity is characterised by the well-defined peak at $2\theta = 16.9°$ and by the broad and small peak at $2\theta = 22.0°$. The short-term development of B-type crystallinity in the maize starch films can be attributed to the fast re-crystallization of amylose molecules. B-type crystallinity indices of $x_c \approx 0.49(\pm 0.05)$ and $x_c \approx 0.45(\pm 0.05)$ were

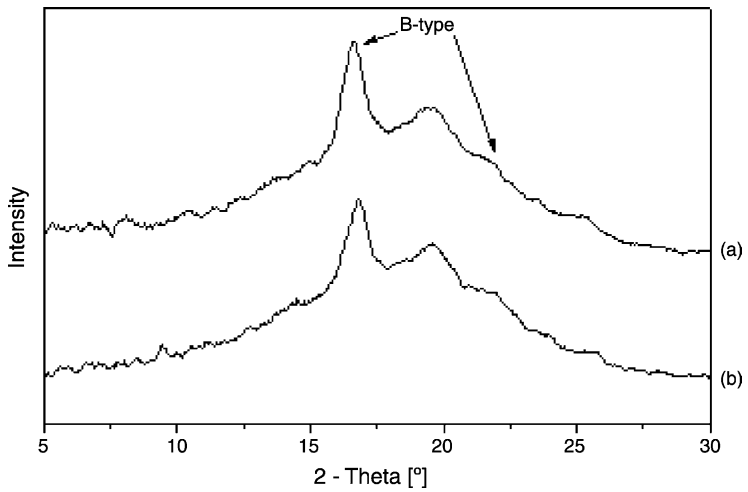

Fig. 4. X-ray diffractograms of plasticised maize starch films: (a) 5MG and (b) 90MG.

determined for the 5MG and 90MG films, respectively, according to the method described in the literature (Hulleman et al., 1999) and are within experimental error.

Higher magnification three-dimensional topographic images of the granular envelope and ghost regions on the surface of glycerol-plasticised films are shown in Fig. 5. It could be noticed that the images had not been taken sequentially, but result from independently scanning of a 5MG (Fig. 5(a)), a 20MG (Fig. 5(b)) and a 90MG (Fig. 5(c)) film. The topographic image of Fig. 5(a) shows a swollen granular envelope, in which the surface seems intact. In this figure, the presence of a depressed interface between the granular envelope and the surrounding matrix is supported.

In Fig. 5(b), differences in height on the scanned surface of the 20MG film revealed a withered ghost, which supports that a great amount of starch molecules had been released into the continuous matrix. Indicated by arrows, a tubular structure with average dimensions of 8 μm in width and

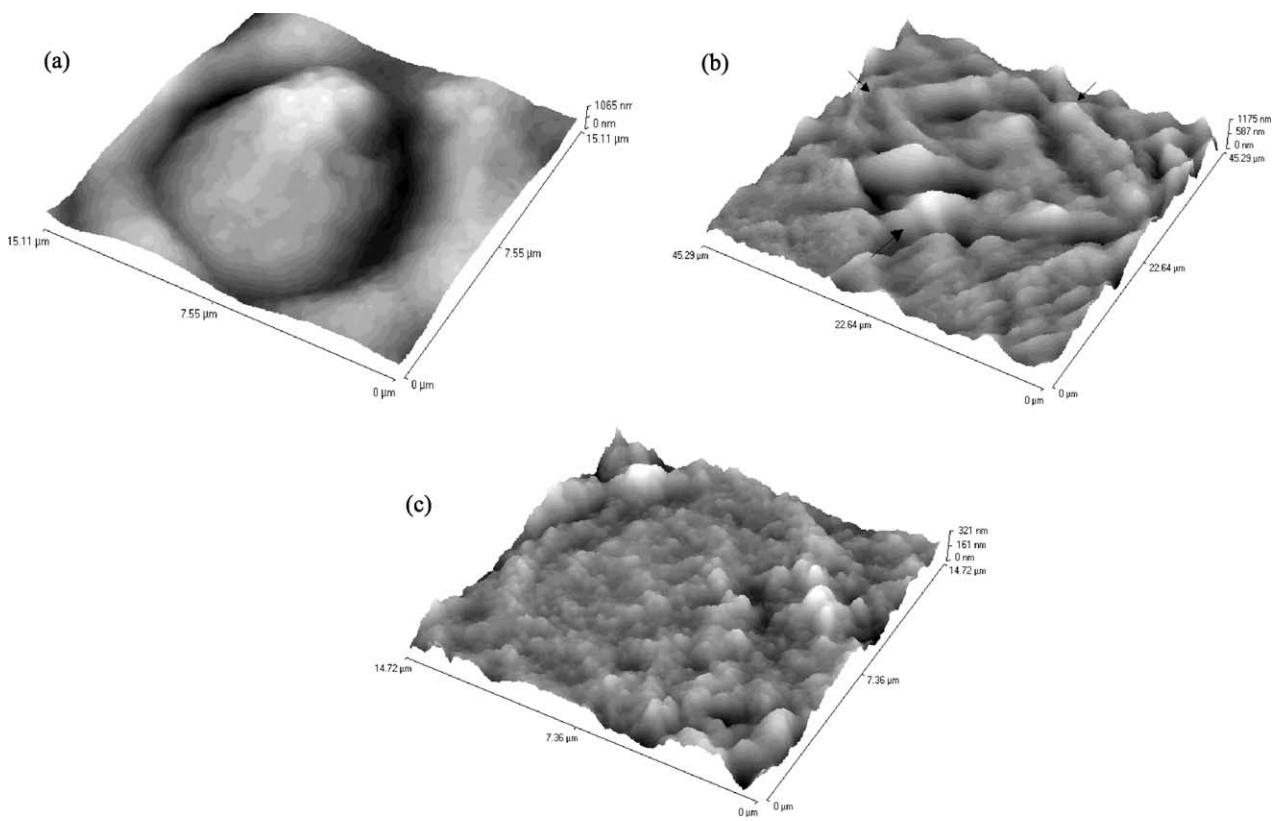

Fig. 5. AFM three-dimensional topographic images of smooth regions on the surface of plasticised maize starch films: (a) 5MG, (b) 20MG, and (c) 90MG.

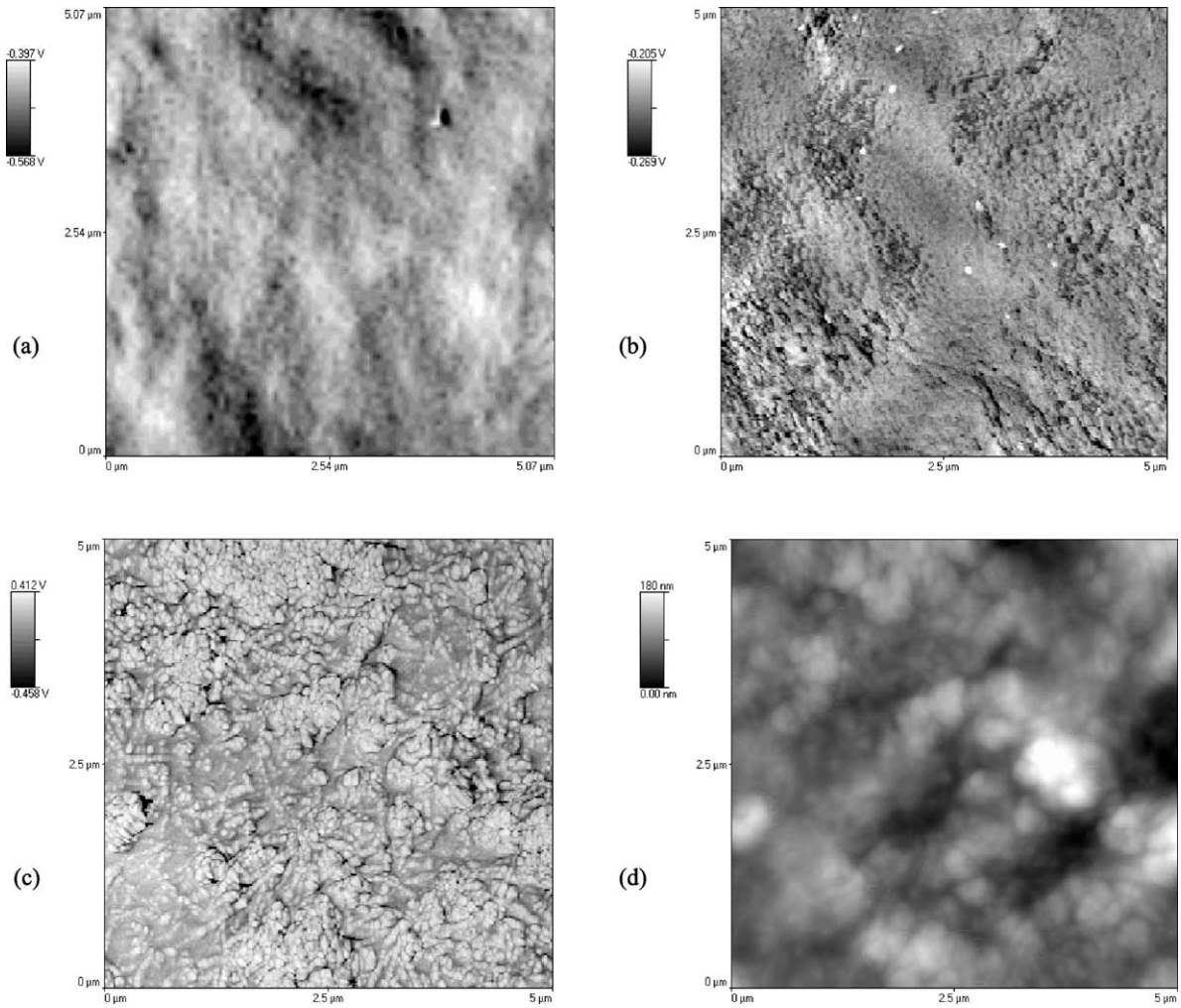

Fig. 6. AFM phase contrast images of smooth regions on the surface of plasticised maize starch films: (a) 5MG, (b) 20MG, (c) 90MG, and (d) AFM topographic image of the same region visualised in (c).

0.2 µm in height may be visualised. Wrinkles and folds have been previously assigned to envelopes of swollen granules, in particular in waxy maize starch (Atkin et al., 1998b). In the present case, there is no evidence whether the ghost structure is ruptured or not.

Differences in height also allowed to identify smooth and rough regions on the surfaces of 90MG films. In every film investigated, smooth regions encircled by nodules of higher heights, which were surrounded by rougher regions, were observed. In Fig. 5(c), one of those smooth regions and nodules are imaged. Comparison of this figure with Fig. 5(b) seems to indicate that these limiting nodules have their origin in the rupture of tubular structures such as that previously imaged on the surface of the 20MG film. Since rough surfaces of similar morphology were also scanned outside granular envelopes of 5MG films and outside withered ghosts of 20MG films, it seems that the 90MG films, although more homogeneous, also consist of a matrix that surrounds ghost remnants.

Intermittent contact mode AFM allows the use of the changes in phase angle of the cantilever probe to produce phase contrast images. These images provide significantly more contrast than topographic images and have been shown to be sensitive to material surface properties, such as stiffness, viscoelasticity and chemical composition (Bar, Thomann, Brandsch, Cantow, & Whangho, 1997; Tamayo & Garcia, 1996). AFM phase contrast images (Fig. 6(a)–(c)) were obtained for the smooth regions of glycerol-plasticised films at higher magnification. No ordered features were imaged on these smooth surfaces at this magnification. However, on a few granular envelopes in 5MG films (images not shown), rough regions attributed to amylose deposition were observed.

According to the images of Fig. 6(a)–(c), the morphology of these surfaces depends on the heating time used for starch gelatinisation. As the heating time increases, the dense and homogeneous structure of the granular envelope surface of the 5MG film (Fig. 6(a)) changes to a more opened structure composed of irregular substructures (Fig. 6(c)). Distinct morphological patterns are evidenced in the phase contrast images obtained for the smooth regions of 20MG and 90MG films. The phase contrast observed in

these figures may be related to the phase separation between the disrupted outer layer of the ghost consisting of amylopectin molecules (Baldwin et al., 1997) and the starch molecules, most probably amylopectin, released from inside the ghosts to the surface of the films. This observation corroborates with the idea supported by some authors that the surface amylopectin differs in some way from internal amylopectin (Atkin et al., 1998b).

In the phase contrast image of Fig. 6(c), substructures of 50–100 nm in size are observed. However, when the topographic image of the same region is analysed (Fig. 6(d)), larger agglomerates are visualised. Other studies should be carried out to explain the nature of these substructures and agglomerates.

Fig. 7 shows AFM topographic and phase contrast images of the continuous, rough phase (matrix) on the surface of a glycerol-plasticised 90MG film. In the topographic image (Fig. 7(a)), some aggregates with differences in height are observed. The sample roughness and its height variation might be hiding other informations. The phase contrast image of Fig. 7(b) reveals well-defined oval and elongated features with approximately 300 nm in major axis and 60 nm in minor axis. It is important to point out that these features are not related to the topographic morphology. In general, changes in phase angle during scanning are related to energy dissipation caused by tip-sample interactions, and can be due to changes in topography, tip-sample molecular interactions, deformation at the tip-sample contact and to experimental conditions (Raghavan et al., 2000). In the present case, phase contrast may be attributed to the enhanced tip-sample adhesion, due to larger contact areas between tip and features boundaries. In Fig. 7(b), the boxes encircle ordered features. These small crystalline domains present in the matrix may be related to the B-type crystallinity detected by XRD (Fig. 4).

A higher magnification of the region on the bottom-right corner of Fig. 7(b) is shown in Fig. 7(c). In this phase image, the crystalline domain can be observed in more detail on

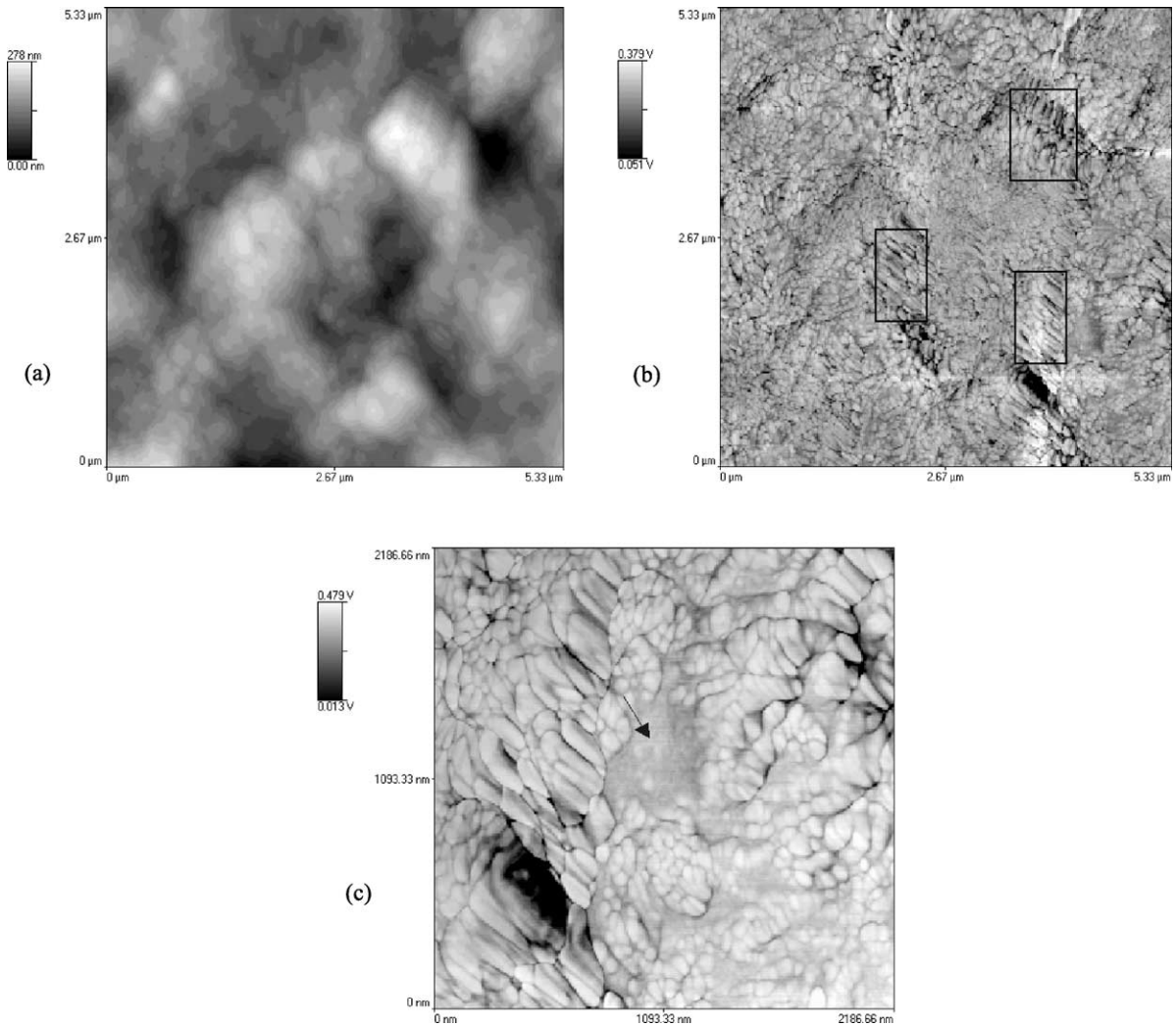

Fig. 7. AFM topographic (a) and phase contrast (b) images of the continuous phase (matrix) on the surface of a 90MG film. (c) Detail of the region on the bottom-right corner of (b).

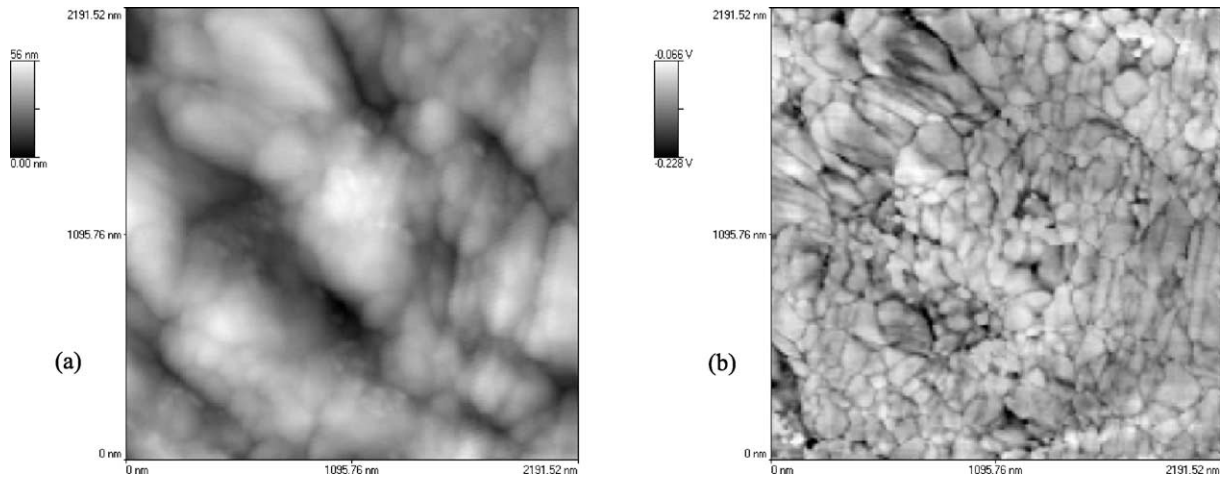

Fig. 8. AFM topographic (a) and phase contrast (b) images of the continuous phase (matrix) on the surface of a non-plasticised maize starch film.

the left side of the figure. The dark region below the crystalline domain may be attributed to a pore, since it is also visualized in the topographic image (Fig. 7(a)). Also in Fig. 7(c), a bright domain indicated by the arrow may be observed at the centre of the magnified area. To explain the nature of this phase, two possibilities should be examined. The first is related to the possible deposition of ghost remnants on the matrix. Due to the reduced size of the domains, this hypothesis should be discarded. The other hypothesis is related to the presence of glycerol-rich phases. Based on dynamical mechanical analysis and dielectric spectroscopy results on barley amylose/glycerol films (Moates, Noel, Parker, & Ring, 2001), the two components were shown to be partially miscible and phase separation was suggested to occur, giving rise to amylose-rich and glycerol-rich phases. The bright phase visualized in Fig. 7(c) might be attributed to a glycerol-rich domain. To support this assumption, matrices of non-plasticised starch films were analysed at the same conditions (Fig. 8). As in Fig. 7(a), the topographic image of Fig. 8(a) provides no special information on structure differences. Contrarily, the phase contrast image (Fig. 8(b)) shows that the matrix is composed of ordered oval and elongated features similar to those observed on the matrix surface of glycerol-plasticised films (Fig. 7(b) and (c)). However, without glycerol, the amylose molecules seems to form greater aggregates, typically 370 nm in major axis and 100 nm in minor axis. No phase separation was observed. Since the matrices of 5MG, 20MG and 90MG films presented the same morphology, and practically no differences were observed in the XRD patterns displayed by the 5MG and 90MG films, the same amylose composition might be postulated to these matrices, independently of the heating time.

4. Conclusions

Differences in surface morphology observed for starch cast films by LM and AFM depend on the preparation conditions. Smooth and rough regions were observed in the AFM topographic images. For plasticised or non-plasticised films, depending on the gelatinisation stage determined by the heating period, images of the smooth regions revealed domains consisting of different features, separated from rough regions by a depression or encircled by nodules of higher height. Variation in the morphology of these features was better visualized by phase contrast imaging. Granular envelopes, ghosts, ghost remnants and non-crystalline substructures were visualized as phase separated domains from the continuous amylose matrix. The morphology of the rough regions or continuous matrix was shown to vary for plasticised and non-plasticised films by phase contrast imaging. For plasticised and non-plasticised films, crystalline domains, resulting from re-crystallisation of amylose, were observed. For plasticised films, the matrix microstructure was similar, independently of the preparation conditions, and bright domains, attributed to glycerol-rich phases, were visualised.

Acknowledgements

The authors would like to thank B.S. Pizzorno for experimental assistance and NUCAT/COPPE/UFRJ for permission to use the X-ray diffractometer. The financial support of Conselho Nacional de Desenvolvimento Científico e Tecnológico (CNPq), Fundação de Amparo à Pesquisa do Estado do Rio de Janeiro (FAPERJ), Fundação Universitária José Bonifácio (FUJB-UFRJ) and PRONEX grant No. 41.96.090900 is also acknowledged.

References

Atkin, N. J., Abeysekera, R. M., Cheng, S. L., & Robards, A. W. (1998a). An experimentally-based predictive model for the separation of

amylopectin subunits during starch gelatinization. *Carbohydrate Polymers*, *36*, 173–192.

Atkin, N. J., Abeysekera, R. M., & Robards, A. W. (1998b). The events to the formation of ghosts remnants from the starch granule surface and the contribution of the granule surface to the gelatinisation endotherm. *Carbohydrate Polymers*, *36*, 193–204.

Baker, A., Miles, M. J., & Helbert, W. (2001). Internal structure of the starch granule revealed by AFM. *Carbohydrate Research*, *330*, 249–256.

Baldwin, P. M., Davies, M. C., & Melia, C. D. (1997). Starch granule surface imaging using low-voltage scanning electron microscopy and atomic force microscopy. *International Journal of Biological Macromolecules*, *21*, 103–107.

Bar, G., Thomann, Y., Brandsch, R., Cantow, H. J., & Whangho, M. H. (1997). Factors affecting the height and phase images in tapping mode atomic force microscopy. Study of phase-separated polymer blends of poly(ethene-co-styrene) and poly(2,6-dimethyl-1,4-phenylene oxide). *Langmuir*, *13*, 3807–3812.

Bastioli, C. (1998). Biodegradable materials—present situation and future perspectives. *Macromolecular Symposium*, *135*, 193–204.

Cooke, D., & Gidley, M. J. (1992). Loss of crystalline and molecular order during starch gelatinisation: Origin of the enthalpic transition. *Carbohydrate Research*, *227*, 103–112.

Derek, R., Prentice, M., Stark, R., & Gidley, M. J. (1992). Granule residues and 'ghosts' remaining after hating A-type barley-starch granules in water. *Carbohydrate Polymers*, *227*, 121–130.

Donovan, J. W. (1979). Phase transitions of the starch–water system. *Biopolymers*, *18*, 263–275.

Fannon, J. E., & BeMiller, J. N. (1992). Structure of corn starch paste and granule remnants revealed by low-temperature scanning electron microscopy after cryopreparation. *Cereal Chemistry*, *69*, 456–460.

French, D. (1984). Organisation of the starch granules. In R. L. Whistler, J. N. BeMiller, & J. F. Paschall (Eds.), *Starch: Chemistry and technology* (pp. 183–247). Orlando: Academic Press.

Gallant, D. J., Bouchet, B., & Baldwin, P. M. (1997). Microscopy of starch: Evidence of a new level of ganule organization. *Carbohydrate Polymers*, *32*, 177–191.

Garcia, R., & Pérez, R. (2002). Dynamic atomic force microscopy methods. *Surface Science Reports*, *47*, 197–301.

Gidley, M. J. (1989). Molecular mechanisms underlying amylose aggregation and gelation. *Macromolecules*, *22*, 351–358.

Hermansson, A.-M., & Svegmark, K. (1996). Developments in the understanding of starch functionality. *Trends in Food Science and Technology*, *7*, 345–353.

Hulleman, S. H. D., Kalisvaart, M. G., Janssen, F. H. P., Feil, H., & Vliegenthart, J. F. G. (1999). Origins of B-type crystallinity in glycerol-plasticised, compression-moulded potato starches. *Carbohydrate Polymers*, *39*, 351–360.

Imberty, A., Chanzy, H., Pérez, S., Buléon, A., & Tran, V. (1988). The double-helical nature of the crystalline part of A-starch. *Journal of Molecular Biology*, *201*, 365–378.

Imberty, A., & Pérez, S. (1988). A revisit to the three-dimensional structure of B-type starch. *Biopolymers*, *27*, 1205–1221.

Jang, J. K., & Pyun, Y. R. (1996). Effect of moisture content on the melting of wheat starch. *Starch/Stärke*, *48*, 48–51.

Jenkins, P. J., Cameron, R. E., & Donald, A. M. (1993). A universal feature in the structure of starch granules from different botanical sources. *Starch/Stärke*, *45*, 417–420.

Jenkins, P. J., & Donald, A. M. (1998). Gelatinisation of starch: A combined SAXS/WAXS/DSC and SANS study. *Carbohydrate Polymers*, *308*, 133–147.

Kalichevsky, M. T., & Ring, S. G. (1987). Incompatibility of amylose and amylopectin in aqueous solution. *Carbohydrate Research*, *162*, 323–328.

Kassenbeck, P. (1975). Electronenmikroskopisher beitrag zur kenntnis der feinstruktur der weizenstärke. *Starch/Stärke*, *27*, 217–227.

Kassenbeck, P. (1978). Beitrag zur kenntnis der verteilung von amylose und amylopektin in stärkekörnern. *Starch/Stärke*, *30*, 40–46.

Keetels, C. J. A. M., Oostergetel, G. T., & van Vliet, T. (1996). Recrystallization of amylopectin in concentrated starch gels. *Carbohydrate Polymers*, *30*, 61–64.

Krok, F., Szymonska, J., Tomasik, P., & Szymonski, M. (2000). Non-contact AFM investigation of the influence of freezing process on the surface structure of potato starch granule. *Applied Surface Science*, *157*, 382–386.

Kuutti, L., Peltonen, J., Myllärinen, P., Teleman, O., & Forssell, P. (1998). AFM in studies of thermoplastic starches during ageing. *Carbohydrate Polymers*, *37*, 7–12.

Lörks, J. (1998). Properties and applications of compostable starch-based plastic material. *Polymer Degradation and Stability*, *59*, 245–249.

Miles, M. J., Morris, V. J., Orford, P. D., & Ring, S. G. (1985). The roles of amylose and amylopectin in the gelation and retrogradation of starch. *Carbohydrate Polymers*, *135*, 271–281.

Miller, B. S., Derby, R. I., & Trimbo, H. B. (1973). A pictorial explanation for the increase in viscosity of a heated starch–water suspension. *Cereal Chemistry*, *50*, 271–280.

Moates, G. K., Noel, T. R., Parker, R., & Ring, S. G. (2001). Dynamic mechanical and dielectric characterisation of amylose–glycerol films. *Carbohydrate Polymers*, *44*, 247–253.

Obanni, M., & BeMiller, J. N. (1996). Ghost microstructures of starch from different botanical sources. *Cereal Chemistry*, *73*, 333–337.

Oostergetel, G. T., & van Bruggen, E. F. J. (1989). On the origin of a low angle spacing in starch. *Starch/Stärke*, *41*, 331–335.

Perry, P. A., & Donald, A. M. (2000). The role of plasticization in starch granule assembly. *Biomacromolecules*, *1*, 424–432.

Raghavan, D., & Emekalam, A. (2001). Characterization of starch/polyethylene and starch/polyethylene/poly(lactic acid) composites. *Polymer Degradation and Stability*, *72*, 509–517.

Raghavan, D., Gu, X., Nguyen, T., VanLandingham, M., & Karim, A. (2000). Mapping polymer heterogeneity using atomic force microscopy phase imaging and nanoscale indentation. *Macromolecules*, *33*, 2573–2583.

Ridout, M. J., Gunning, A. P., Parker, M. L., Wilson, R. H., & Morris, V. J. (2002). Using AFM to image the internal structure of starch granules. *Carbohydrate Polymers*, *50*, 123–132.

Rindlav, A., Hulleman, S. H. D., & Gatenholm, P. (1997). Formation of starch films with varying crystallinity. *Carbohydrate Polymers*, *34*, 25–30.

Rindlav-Westling, A., Stadin, M., Hermansson, A.-M., & Gatenholm, P. (1998). Structure, mechanical and barrier properties of amylose and amylopectin films. *Carbohydrate Polymers*, *36*, 217–224.

Shogren, R. L. (1993). Effects of moisture and various plasticizers on the mechanical properties of extruded starch. In C. Ching, D. L. Kaplan, & E. L. Thomas (Eds.), *Biodegradable polymers and packaging* (pp. 141–150). Lancaster: Technomic Publishing Company.

van Soest, J. J. G., Hulleman, S. H. D., de Witt, D., & Vliegenthart, J. F. G. (1996). Crystallinity in starch bioplastics. *Industrial Crops and Products Technology*, *5*, 11–22.

Stokke, B. T., & Elgsaeter, A. (1991). Electron microscopy of carbohydrate polymers. In C. A. White (Ed.), *Advances in Carbohydrate Analysis* (pp. 195–247). Birmingham: JAI Press.

Tamayo, J., & Garcia, R. (1996). Deformation, contact time, and phase contrast in tapping mode scanning force microscopy. *Langmuir*, *12*, 4430–4435.

Yamaguchi, M., Kainuma, K., & French, D. J. (1979). Electron microscopic observations of waxy maize starch. *Journal of Ultrastructure Research*, *69*, 249–261.